Angewandte
Zuschriften

Iron Heterocubanes

Deutsche Ausgabe: DOI: 10.1002/ange.201505668
Internationale Ausgabe: DOI: 10.1002/anie.201505668

A Low-Valent Iron Imido Heterocubane Cluster: Reversible Electron Transfer and Catalysis of Selective C–C Couplings

Crispin Lichtenberg, Inés Garcia Rubio, Liliana Viciu, Mario Adelhardt, Karsten Meyer, Gunnar Jeschke, and Hansjörg Grützmacher**

Dedicated to Professor Herbert W. Roesky on the occasion of his 80th birthday

Abstract: *Enzymes and cofactors with iron–sulfur heterocubane core structures, [Fe_4S_4], are often found in nature as electron transfer reagents in fundamental catalytic transformations. An artificial heterocubane with a [Fe_4N_4] core is reported that can reversibly store up to four electrons at very negative potentials. The neutral [Fe_4N_4] and the singly reduced low-valent [Fe_4N_4]$^-$ heterocubanes were isolated and fully characterized. The low-valent species bears one unpaired electron, which is localized predominantly at one iron center in the electronic ground state but fluctuates with increasing temperatures. The electrons stored or released by the [Fe_4N_4]/[Fe_4N_4]$^-$ redox couple can be used in reductive or oxidative C–C couplings and even allow catalytic one-pot reactions, which show a remarkably enhanced selectivity in the presence of the [Fe_4N_4] heterocubanes.*

Iron–sulfur clusters with a heterocubane core geometry (Fe_4S_4) are ubiquitous electron storage sites in enzymes and cofactors.[1,2] Prominent examples include nitrogenases[3] and hydrogenases,[4] in which Fe_4S_4 clusters are involved as electron relays in fundamental catalytic transformations, such as activation of N_2 and H_2. The iron centers in Fe_4S_4 change their oxidation states between Fe^{II} and Fe^{III}, which in principle allows uptake and release of up to four electrons in remarkably small volumes of ca. 2.3–2.6 Å^3.[5,6] The redox potentials are crucial for the type of catalytic transformation that can be performed and typically range from ca. −0.1 V to −1.4 V vs. ferrocene/ferrocenium (Fc/Fc^+) in biologically relevant Fe_4S_4 based systems.[1,7] The fascinating properties of Fe_4S_4 clusters have stimulated an intensive search for artificial iron heterocubanes [$Fe_4Q_4L_4$], which have been studied in great detail. The accessible potential range and the number of chemically reversible redox events can be modified to a greater extent in these [$Fe_4Q_4L_4$] clusters with Q = O,[8–10] S,[11–19] Se,[20,21] NR,[22–27] S/NR,[28–31] CO;[16,32–34] L = neutral or anionic ligand (see the Supporting Information for details). Up to four chemically reversible redox events are possible for two systems with Q = O[8–10] or S[19] in a potential range of ca. −0.4 to −1.4 V and +0.9 to −0.7 V, respectively. [Fe_4S_4-($S t Bu$)$_4$] shows three quasi-reversible redox events, with one at a very low potential of about −2.6 V.[14,15] Some insight in the stoichiometric reactivity of [$Fe_4Q_4L_4$] has been gained,[22,23,35,36] but only very few examples for catalytic applications have been reported.[37]

Trop-substituted amines (trop = 5*H*-dibenzo[*a*,*d*]cyclohepten-5-yl) have been reported to stabilize transition metals in unusual low oxidation states owing to their steric and electronic properties.[38,39] Herein, we report the new iron/nitrogen heterocubane [$Fe_4(Ntrop)_4$], which can reversibly store up to four electrons at very low redox potentials. These processes involve four consecutive formal Fe^{II}/Fe^{I} redox couples of which the mono-reduced derivative [$Fe_4(Ntrop)_4$]$^-$ was isolated with Na^+ or [$Co(C_5Me_5)_2$]$^+$ as counter cations.

In a fast reaction, the intensely dark-brown iron imide [$Fe_4(Ntrop)_4$] (**1**) is assembled in good yield by simply mixing [$Fe(NCy_2)_2$] (Cy = cyclohexyl) with H_2Ntrop at room temperature in toluene (Scheme 1). Reduction of **1** with either [$Co(C_5Me_5)_2$] or Na/Hg affords the singly reduced compounds [$Co(C_5Me_5)_2$]$^+$[Fe_4Ntrop_4]$^-$ (**2a**) and [$Na(thf)_4$]$^+$[Fe_4Ntrop_4]$^-$ (**2b**), respectively, in quantitative yields (from spectroscopy)

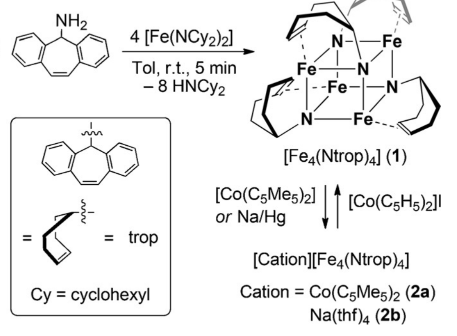

Scheme 1. Synthesis of heterocubane [$Fe_4(Ntrop)_4$] (**1**) and the singly reduced derivatives [$Co(C_5Me_5)_2$]$^+$[$Fe_4(Ntrop)_4$]$^-$ (**2a**) and [$Na(thf)_4$]$^+$-[$Fe_4(Ntrop)_4$]$^-$ (**2b**).

---

[*] Dr. C. Lichtenberg, Dr. I. Garcia Rubio,[+] Dr. L. Viciu,
Prof. Dr. G. Jeschke, Prof. Dr. H. Grützmacher
Department of Chemistry and Applied Biosciences, ETH Zürich
Vladimir-Prelog-Weg 1, 8093 Zürich (Switzerland)
E-mail: hgruetzmacher@ethz.ch
M. Adelhardt, Prof. Dr. K. Meyer
Department of Chemistry & Pharmacy
Friedrich-Alexander University, Erlangen—Nürnberg (FAU)
Egerlandstrasse 1, 91058 Erlangen (Germany)
[+] Current address: Centro Universitario de la Defensa,
Academia General Militar
Crta. de Huesca s/n, Zaragoza, 50090 (Spain)

Supporting information and ORCID(s) from the author(s) for this article are available on the WWW under http://dx.doi.org/10.1002/anie.201505668.

and moderate yields (isolated). Compounds **1** and **2** are air-sensitive, but stable under inert atmosphere in the solid state (>90 d, −30 °C) and in solution (>5 d, RT, benzene (for **1**) or THF (for **2b**)).

Single-crystal X-ray analysis of **1** revealed a heterocubane structure with each olefinic group, C=C^{trop}, of the (Ntrop)$^{2-}$ ligand coordinated to one iron center (Scheme 1, Figure 1 a). Whereas iron imides with heterocubane structures $[Fe_4(NR)_4]^n$ (R = alkyl, aryl) have been reported for $n = 5+$, $4+$, $3+$, $2+$,[22–26] compound **1** is the first example of such a species with $n = 0$, that is, all four iron centers are ferrous (for related $[Fe_4(NPR_3)_4(X)_4]$ compounds (X = Cl, CCSiMe$_3$), see Ref. [40]). Overall, the gross structure of the Fe_4N_4 core in **1** is similar to that of known Fe_4N_4 heterocubanes, as reflected by comparable Fe-N-Fe, N-Fe-N, and Fe-Fe-Fe angles. However, the Fe−N and Fe−Fe distances in **1** (average: 1.912(7) Å and 2.4798(15) Å) are shorter compared to other iron imido heterocubanes (average: 1.95–1.99 Å and 2.61–2.69 Å).[6] Consequently, the volume of the Fe_4 tetrahedron in **1** (1.801(3) Å^3) is reduced by 14–22%. We ascribe this size reduction to the chelating effect of the (Ntrop)$^{2-}$ ligand and to the π-acidity of its coordinating olefinic group, which induces substantial direct Fe−Fe bonding in **1** (see below).

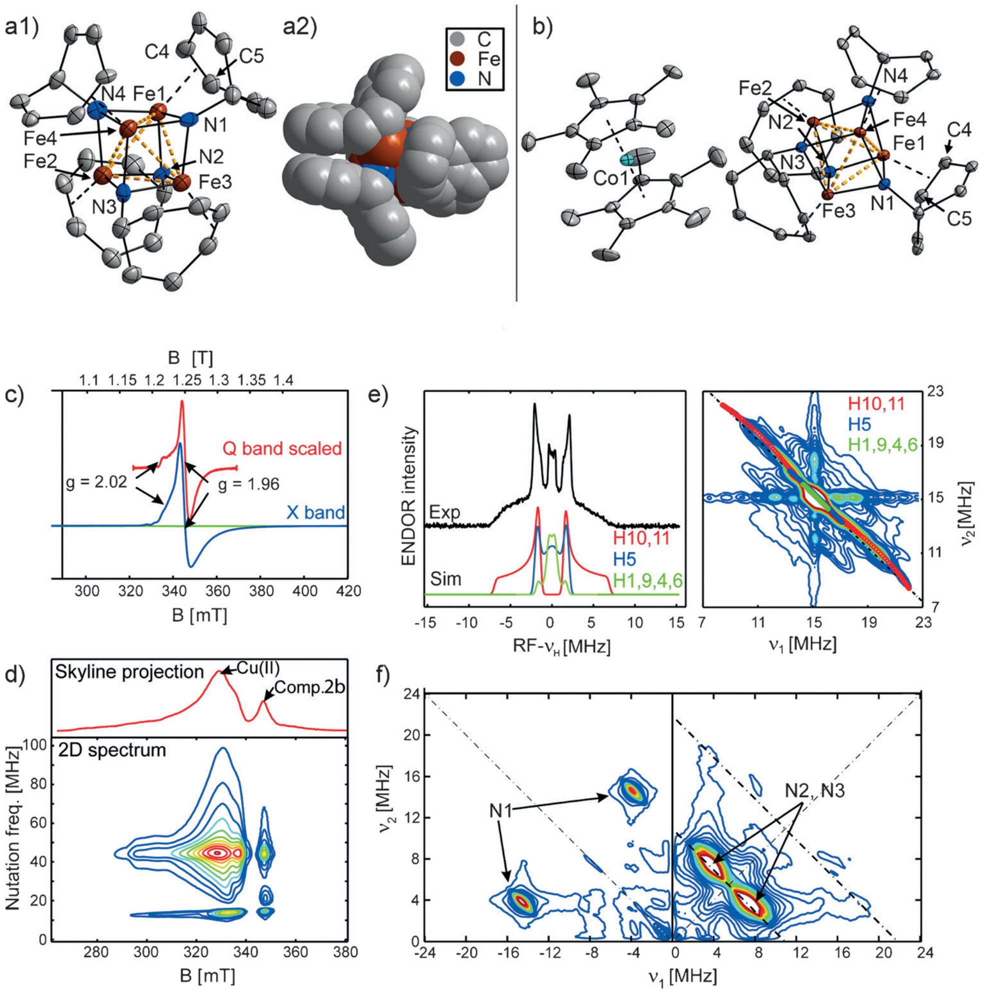

Figure 1. Solid-state structures: a1) Molecular structure of $[Fe_4(Ntrop)_4]\cdot(thf)_{3.3}$ ($\mathbf{1}\cdot(thf)_{3.3}$) and corresponding space-filling model with H atoms and THF molecules in the lattice omitted for clarity (a2).[53] b) Molecular structure of $[Co(C_5Me_5)_2]^+[Fe_4(Ntrop)_4]^-\cdot(NC_5H_5)_4$ [$\mathbf{2a}\cdot(NC_5H_5)_4$].[53] Ellipsoids are set at 50% probability; hydrogen atoms, annelated C_6H_4 groups, and solvent molecules in the lattice are omitted for clarity. Selected bond lengths [Å] and angles [°]: **1**: Fe1−N1 1.924(6), Fe1−N2 1.952(6), Fe1−N4 1.908(6), Fe1−ct(C4−C5) 1.928(7), C4−C5 1.416(10), Fe1−Fe2 2.4982(14), Fe1−Fe3 2.4781(15); Fe2-Fe1-Fe3 59.24(4), N1-Fe1-N2 98.2(2). **2a**: Fe1−N1 1.920(3), Fe1−N2 1.929(3), Fe1−N4 1.922(3), Fe1−ct(C4−C5) 1.912(4), C4−C5 1.431(6), Fe1−Fe3 2.4630(7), Fe2−Fe3 2.5232(7); Fe2-Fe1-Fe3 60.87(2), N1-Fe1-N4 98.76(12). EPR spectroscopy: c) X-band CW-EPR spectra of **1** (green line) and **2b** (blue line). The red spectrum and the upper axis correspond to the scaled Q-band spectrum of **2b**; $T = 10$ K. d) Nutation frequency recorded as a function of the magnetic field in X-band for a sample containing **2b** and an aqueous solution of a Cu^{II} standard with $S = 1/2$. e) Interactions with protons in **2b**. Davies ENDOR (left panel) and HYSCORE spectra (right panel) at $T = 10$ K. The signals for different surrounding protons were simulated using the parameters collected in the supplementary information. f) Q-band HYSCORE spectrum of ^{15}N-labeled **2b** showing features corresponding to one plus two nitrogen nuclei. To avoid the effect of blind spots, the displayed spectrum corresponds to the sum of spectra at three different τ values. For ENDOR and HYSCORE experiments, the magnetic field was selected at the maximum of absorption ($g = 1.96$).

The structure of the reduced $[Co(C_5Me_5)_2]^+[Fe_4(Ntrop)_4]^-$ (**2a**) was also determined by a single-crystal X-ray analysis (Figure 1 b). There are no short directed interactions between cations and anions, and the heterocubane structure is maintained. The four iron centers Fe1−Fe4 in **2a** show similar bonding parameters indicating delocalization of the additional electron as has been observed in Fe^{2+}/Fe^{3+} mixed valence iron imido heterocubanes.[12,23,25] In comparison to **1**, the reduced $[Fe_4(Ntrop)_4]^-$ cube in **2a** shows consistently larger Fe−Fe ($\Delta_{avg} = 0.02$ Å), Fe−N ($\Delta_{avg} = 0.02$ Å), and C=C^{olefin} ($\Delta_{avg} = 0.02$ Å) distances. Concomitantly the Fe−(C=C^{trop}) distances are shorter ($\Delta_{avg} = -0.01$ Å), indicating efficient electron back-donation from the iron centers to the olefinic groups (see the Supporting Information).

Compounds **1**, **2a**, and **2b** were investigated by zero-field ^{57}Fe Mössbauer spectroscopy at 77 K (Supporting Information). **1** shows a quadrupole doublet with $\delta = 0.30(1)$ mm s^{-1} and $|\Delta E_Q| = 1.78(1)$ mm s^{-1}, thus ruling out a high-spin electron configuration, which was reported for the few other iron imido heterocubanes.[23,25,27] This supports the presence of Fe−Fe bonds in compound **1**. The quadrupole splitting of **1** is larger than that of Fe^{3+} or Fe^{2+}/Fe^{3+} imido heterocubanes ($|\Delta E_Q| = 0.55$–$1.32\ mm\,s^{-1}$), which is attributed to the chelating character of the $(Ntrop)^{2-}$ ligand. Reduced **2a** and **2b** show each one quadrupole doublet indicating that the additional electron (compared to **1**) is delocalized in the cluster at 77 K on the time scale of the Mössbauer spectroscopic experiment. This is in agreement with the results obtained from single-crystal X-ray analyses at 100 K (see above). Identical isomer shifts ($0.33(1)\ mm\,s^{-1}$) and very similar quadrupole splittings ($|\Delta E_Q| = 1.35(1), 1.31(1)\ mm\,s^{-1}$) were observed for **2a** and **2b**, revealing that the counterion ($[(Co(C_5Me_5)_2]^+$ vs. $[Na(thf)_4]^+$) does not have a substantial effect on the Mössbauer parameters. The quadrupole splittings are moderately decreased compared to **1**. The small but significant increase in the isomer shift suggests that the effect of longer Fe−N bonds slightly overcompensates the effect of shorter Fe−C bonds in **2a/b** compared to **1**.

Compounds **1**, **2a**, and **2b** were analyzed by SQUID magnetization measurements in an applied field of 1 T (Supporting Information). At 300 K they show effective magnetic moments of $\mu_{eff} = 2.83\ \mu_B$ (**1**), and 2.27–2.30 μ_B (**2a**,**b**), respectively. With decreasing temperature, μ_{eff} steadily decreases to reach values of 0.77 μ_B (**1**) and 1.64–1.54 μ_B (**2a**,**b**). These findings indicate intramolecular antiferromagnetic interactions as previously described for iron–sulfur clusters with heterocubane structures.[41] Overall, the magnetic susceptibility data indicate $S = 0$ and $S = 1/2$ ground states for **1** and **2a/b**, respectively, with higher electronic states being increasingly populated with increasing temperature. In all cases, the experimental data were best reproduced in simulations using antiferromagnetic spin-coupling models in which one Fe center shows parameters different from the other three Fe centers. Local spin states of $4 \times S = 1$ (for **1**) and $3 \times S = 1$ plus $1 \times S = 1/2$ (for **2a,b**) were assumed, and best-fit simulations give antiferromagnetic coupling constants $J = -174\ cm^{-1}$, $J' = -94\ cm^{-1}$ (for **1**) and $J = -244/-195\ cm^{-1}$, $J' = -244/-244\ cm^{-1}$ (for **2a/b**) (Supporting Information). It should be noted that the existence of a diamagnetic ground state has been under debate for all-ferrous $[Fe_4S_4]$ clusters in biological systems.[42,43] The solution effective magnetic moments at 298 K of **1** (C_6D_6, 2.7(1) μ_B) and **2b** ($[D_8]$THF, 2.4(2) μ_B) determined by Evans' method are close to those determined in the solid state, giving evidence for the solid-state structures being essentially maintained in solution. There are no experimental indications that **1** or **2** dissociate into dinuclear subunits.[24,26]

Compound **1** is EPR-silent in a 2-MeTHF glass at 10 K, which is in agreement with an $S = 0$ ground state (Figure 1c, green line). Compound **2b** shows an axial X-band EPR signal without any resolved hyperfine coupling in a 2-MeTHF glass at 10 K ($g_\parallel = 2.02$; $g_\perp = 1.96$), which is consistent with S_4 symmetry in solution (Figure 1c). An electron spin echo was detected from the reduced compound **2b**, and its $S = 1/2$ ground state at $T = 10$ K was confirmed by comparison with a Cu^{II} standard in two-dimensional EPR spectroscopic nutation experiments (Figure 1d). Davies ENDOR and HYSCORE experiments reveal the interaction of several protons with the electron spin (Figure 1e). The estimation of the different proton hyperfine anisotropies based on the through-space point-dipole interaction using the Fe⋯H distances (derived from the single-crystal X-ray analysis of **2a**) yielded values very close to those observed in the spectra. This indicates localization of the unpaired electron at one FeNtrop subunit in a distorted Fe_4N_4 cube rather than delocalization over the entire cluster. Remarkably, HYSCORE experiments at 10 K on **2b** and ^{15}N-labeled **2b** (Figure 1 f) reveal strong coupling with one nitrogen nucleus (N1, with $A^1 \approx 18$ MHz) and interactions in the weak coupling regime with two nitrogen atoms (N2 and N3, with $A^{2,3} \approx 4$ MHz), which is again consistent with localization of the unpaired electron. This phenomenon was not resolved by other analytical techniques (VT NMR, Mössbauer spectroscopy, X-ray diffraction), which is due to their lower time resolution and the higher temperatures at which these measurements were performed (77–300 K). Additionally, HYSCORE spectra revealed weak couplings with carbon nuclei (Supporting Information). Thus the analysis of the hyperfine interactions of the unpaired electron with the surrounding magnetic nuclei reveals that the unpaired electron in **2b** is predominantly located at one Fe center (spin density $\rho \approx 80\%$) with some delocalization to the coordinated $C{=}C^{Olefin}$ unit ($\rho \approx 18\%$) and to the nitrogen atom that is part of the same chelating ligand ($\rho \approx 0.8\%$). Only minor contributions to the total spin density are detected at the other two nitrogen nuclei that directly interact with the Fe radical center ($\rho \approx 0.2\%$ each; Supporting Information). This is in contrast to the electronic structure of $[M(Ntrop_2)(bipy)]^+$ (M = Rh, Ir), where the spin is predominantly located at the nitrogen center, leading to a description as stable cationic aminyl radical complexes.[44,45]

Cyclic voltammetry of **1** in THF at 23 °C revealed four chemically reversible redox events, which are assigned to the electron-transfer series denoted in Figure 2.[46] The redox processes take place between −1.72 and −3.59 V vs. Fc/Fc^+, which is the most negative potential range reported for iron heterocubanes. Note that the shapes of the curves for the redox events E_3 and E_4 are affected by the onset of reductive solvent decomposition.[47] The chemical reversibility in the cyclic voltammogram of **1** shows that the cluster can store up to four electrons and remains intact in solution over five distinct oxidation states, which is comparable to some iron heterocubanes with oxygen[8] or sulfur[19] as heteroatoms. The large difference of up to 870 mV between the potentials of consecutive redox events E_1–E_4 suggests strong electronic coupling between the metal centers, especially for E_1/E_2.[48] In agreement with the electron-transfer series depicted in Figure 2 (bottom), compound **1** did not react with $[Co(C_5H_5)_2]$ ($E^{0\prime} \approx -1.3$ V), and stronger reducing agents such as $[Co(C_5Me_5)_2]$ ($E^{0\prime} \approx -1.9$ V) were necessary to obtain the singly reduced species **2**. Oxidation of **2a** with $[Co(C_5H_5)_2]I$ cleanly regenerates compound **1**.

At room temperature, ^{1}H NMR spectra of **1** in $[D_8]$THF show eleven paramagnetically shifted resonances of equal intensity (one pair is overlapping) in the range of about 6–60 ppm. This is in agreement with an apparent S_4 symmetry

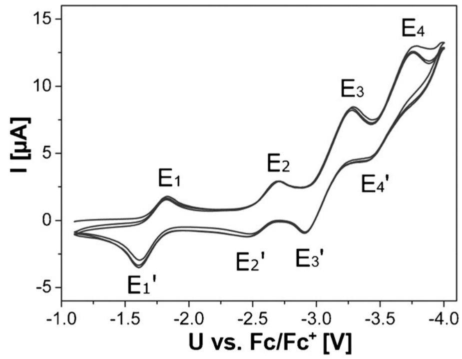

$$[\mathrm{Fe_4(Ntrop)_4}]^{0} \xrightleftharpoons{-1.72\ \mathrm{V}} [\mathrm{Fe_4(Ntrop)_4}]^{1-} \xrightleftharpoons{-2.59\ \mathrm{V}} [\mathrm{Fe_4(Ntrop)_4}]^{2-}$$

$$\xrightleftharpoons{-3.10\ \mathrm{V}} [\mathrm{Fe_4(Ntrop)_4}]^{3-} \xrightleftharpoons{-3.59\ \mathrm{V}} [\mathrm{Fe_4(Ntrop)_4}]^{4-}$$

Figure 2. Cyclic voltammogram of **1** in THF/0.1 M [nBu$_4$N][PF$_6$] versus Fc/Fc$^+$ at 50 mV s^{-1} scan rate (top) at 23 °C, and associated electron transfer series (bottom).

and the cubic structure of the Fe$_4$N$_4$ cluster. The same holds for the reduced species **2a**,**b**, but the ^{1}H NMR resonances are spread over a larger range of about 2–76 ppm (Supporting Information). Upon cooling samples of **1** and **2b** in [D$_8$]THF to 193 K, the chemical shift range of the resonances gradually shrinks to about 6–36 ppm in the case of **1**, in agreement with a diamagnetic S = 0 ground state, but increases to about 2–95 ppm in the case of paramagnetic **2b**. ^{1}H NMR spectroscopic analyses of samples containing mixtures of **1** and **2b** at 23 °C show only one set of signals with averaged chemical shifts. From the ^{1}H NMR spectrum of a 1:1 mixture of **1** and **2b** in [D$_8$]THF at 23 °C (c = 6 mM), an exchange rate $k > 3.2 \times 10^4$ Hz was estimated for the electron transfer (for an investigation of the electron exchange in [Fe$_4$S$_4$(SR)$_4$]$^{3-/2-}$ see Ref. [49]). Upon lowering the temperature to 203 K, broadening of the signals but no decoalescence was observed.

The application of artificial Fe$_4$Q$_4$ heterocubanes as catalysts or electron transfer mediators in organic reactions is rare.[37] In a stoichiometric reaction with n-butyllithium as the reducing agent, [N(nBu)$_4$]$_2$[Fe$_4$S$_4$(SPh)$_4$] mediates the reductive dimerization of fluorenone to bifluoren-9-yl-9,9′-diol in frozen pentane/Et$_2$O solution with moderate selectivity (62 %).[50] The concomitant formation of n-octane showed a lower selectivity of 36 %. The role of the Fe$_4$S$_4$ cluster is unknown. In view of the chemical reversibility of the [Fe$_4$(Ntrop)$_4$]/[Fe$_4$(Ntrop)$_4$]$^-$ redox couple, we investigated this system as an electron-transfer catalyst for C–C bond couplings. Reaction of [Fe$_4$(Ntrop)$_4$] with a slight excess of [Mg(C$_3$H$_5$)Br] (**3**) in THF at 23 °C resulted in the complete conversion into the reduced species [Fe$_4$(Ntrop)$_4$]$^-$ and the coupling product 1,5-hexadiene (**4**) in less than 10 minutes without the formation of detectable side products (Scheme 2, top). Remarkably, compound **1** can also be reduced by sodium alcoholates to give compound **2b**, albeit at slower rates compared to the reaction with **3**. The fate of the alkoxy radicals that are presumably generated is presently unknown. In a separate reaction, the reduced species [Fe$_4$(Ntrop)$_4$]$^-$ was reacted with a slight excess of N-methyl-acridinium iodide, (AcrH)I (**5**), in THF at 23 °C. Clean conversion into the oxidized cluster [Fe$_4$(Ntrop)$_4$] (**1**) and the coupling product N,N'-dimethyl-bis(9,10-dihydro)acridin-9-yl (**6**) was observed in a short time (< 10 min; Scheme 2, bottom). Control experiments showed that direct reaction of [Mg(C$_3$H$_5$)Br] (**3**) with (AcrH)I (**5**) results in the expected allylation of the acridinium ion in the 9-position to give N-methyl-9-(C$_3$H$_5$)-dihydroacridine (**7**) in 93 % yield. The reaction of **5** with NaOtBu likewise gives the expected product of a nucleophilic attack in the 9-position, and **6** was not detected. These results show that with **1** as an electron-transfer mediator, even alcoholate anions can be utilized as reducing agents for reductive C–C coupling reactions. The oxidative coupling of **3** and the reductive coupling of **5** could be performed in a catalytic process if the formation of **7** is suppressed. Indeed, the reaction of [Mg(C$_3$H$_5$)Br] (**3**) with (AcrH)I (**5**) in the presence of 2 mol % **1** in THF at 23 °C gave the symmetrical coupling products 1,5-hexadiene (**4**) and (AcrH)$_2$ (**6**) in 55 % and 38 % yield, respectively, with **7** as a side product (45 % yield). Small amounts of the catalyst in its oxidized form **1** could be detected by NMR spectroscopy after the catalytic experiment. The same reactions with [Co(C$_5$H$_5$)$_2$] or [Co(C$_5$Me$_5$)$_2$] as potential catalysts gave the unsymmetrical coupling product **7** in ca. 80 % yield with only minor amounts of **4** (10 %) and **6** (≤ 3 %).

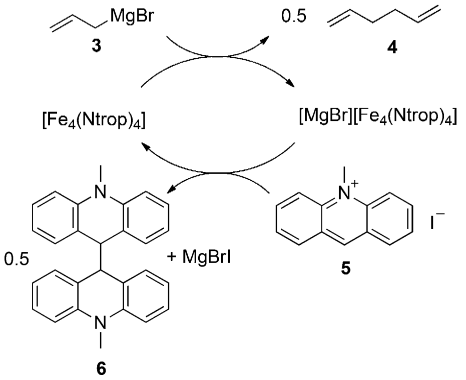

Scheme 2. Catalytic cycle for oxidative dimerization of (C$_3$H$_5$)$^-$ and reductive dimerization of N-methylacridinium ion (AcrH)$^+$ catalyzed by 2 mol % of **1**.

In summary, the synthesis of the easily accessible [Fe$_4$(Ntrop)$_4$] (**1**) was achieved which exists in five distinct oxidation states at very negative electrochemical potentials. According to the effective atomic number (EAN) rule, we propose to describe the 56-valence-electron Fe$_4$ unit in **1** as a hyper-electron-deficient tetrahedral cluster (Supporting Information). The triangular faces of such a cluster core are exclusively formed by three-center–two-electron (3c-2e) bonds.[51] This description of **1** is in agreement with the structure showing short Fe–Fe bonds and with the magnetization data (four unpaired electrons per Fe$^{\mathrm{II}}$ center, of which two are used for bonding in the Fe$_4$ cluster to give a local spin $S = 1$). Reduction perturbs the cluster structure until after addition of four electrons the electron-precise cluster [Fe$_4$(Ntrop)$_4$]$^{4-}$ is formed with a 60-valence-electron Fe$_4$ unit in which each Fe–Fe edge corresponds to a two-center–two-electron (2c-2e) bond. A similar argumentation has been brought forward in a computational modeling study for $[Fe_4S_4(NO)_4]$ in which the Fe_4 unit likewise contains 60 valence electrons.[52] We propose that between the delocalized Fe_4 cluster in **1** with four 3c-2e Fe–Fe–Fe bonds and the localized structure in fully reduced $[\mathbf{1}]^{4-}$ with six 2c-2e Fe–Fe bonds, dynamically disordered localized structures exist for the partially reduced species (as shown for singly reduced **2**).

In a catalytic application, we used the redox couple $[Fe_4(Ntrop)_4]/[Fe_4(Ntrop)_4]^-$ to selectively catalyze the oxidative coupling of allyl anions and the reductive coupling of *N*-methyl-acridinium cations as examples for C–C bond forming reactions. This is a proof-of-principle that the electrons gained in the oxidative coupling simplified as: $2\,A^- + 2\,[Fe_4(Ntrop)_4]$ (**1**)$\rightarrow$A–A $+ 2\,[Fe_4(Ntrop)_4]^-$ (**2**) can be stored and used later and in a different reaction, simplified as: $2\,B^+ + 2\,[Fe_4(Ntrop)_4]^- \rightarrow$B–B $+ 2\,[Fe_4(Ntrop)_4]$ (**1**). These findings demonstrate that using Fe_4Q_4 iron heterocubanes to catalyze bond forming and cleavage processes by reversible storage of electrons, as found in nature, can be transferred to purely artificial systems. We believe that these findings may permit access to new types of designed reactions in which bond forming and breaking events associated with electron-transfer steps can be resolved in time and space.

Acknowledgements

C.L. is grateful for a Feodor Lynen fellowship generously hosted by Prof. François Diederich.

Keywords: C–C coupling · cluster compounds · heterocubanes · homogeneous catalysis · low-valent iron

How to cite: *Angew. Chem. Int. Ed.* **2015**, *54*, 13012–13017
Angew. Chem. **2015**, *127*, 13204–13209

---

[1] M. K. Johnson, K. D. Smith in *Encyclopedia of Inorganic and Bioinorganic Chemistry*, Wiley-VCH, Weinheim, **2011**, pp. 1–31.
[2] H. Beinert, R. H. Holm, E. Münck, *Science* **1997**, *277*, 653–659.
[3] J. B. Howard, D. C. Rees, *Chem. Rev.* **1996**, *96*, 2965–2982.
[4] J. C. Fontecilla-Camps, A. Volbeda, C. Cavazza, Y. Nicolet, *Chem. Rev.* **2007**, *107*, 4273–4303.
[5] R. Holm, *Electron Transfer: Iron-Sulfur Clusters* in *Comprehensive Coordination Chemistry II*, *Vol. 8* (Eds.: L. Que, Jr., W. B. Tolman), Elsevier, Amsterdam, **2003**, pp. 61–90.
[6] L. L. Tan, R. H. Holm, S. C. Lee, *Polyhedron* **2013**, *58*, 206–217.
[7] M. Guo, F. Sulc, M. W. Ribbe, P. J. Farmer, B. K. Burgess, *J. Am. Chem. Soc.* **2002**, *124*, 12100–12101.
[8] R. G. Raptis, I. P. Georgakaki, D. C. R. Hockless, *Angew. Chem. Int. Ed.* **1999**, *38*, 1632–1634; *Angew. Chem.* **1999**, *111*, 1751–1753.
[9] P. Baran, R. Boča, I. Chakraborty, J. Giapintzakis, R. Herchel, Q. Huang, J. E. McGrady, R. G. Raptis, Y. Sanakis, A. Simopoulos, *Inorg. Chem.* **2008**, *47*, 645–655.
[10] A. Masello, Y. Sanakis, A. K. Boudalis, K. A. Abboud, G. Christou, *Inorg. Chem.* **2011**, *50*, 5646–5654.
[11] R. H. Holm in *Comprehensive Coordination Chemistry II*, *Vol. 8* (Eds.: J. A. McCleverty, T. J. Meyer), Elsevier, New York, **2004**, pp. 61–90.
[12] H. Ogino, S. Inomata, H. Tobita, *Chem. Rev.* **1998**, *98*, 2093–2121.
[13] C. R. Sharp, J. S. Duncan, S. C. Lee, *Inorg. Chem.* **2010**, *49*, 6697–6705.
[14] B. V. DePamphilis, B. A. Averill, T. Herskovitz, L. Que, Jr., R. H. Holm, *J. Am. Chem. Soc.* **1974**, *96*, 4159–4167.
[15] P. K. Mascharak, K. S. Hagen, J. T. Spence, R. H. Holm, *Inorg. Chim. Acta* **1983**, *80*, 157–170.
[16] W. E. Geiger, N. G. Connelly in *Advances in Organometallic Chemistry*, *Vol. 24* (Ed.: W. L. Gladfelter), Academic Press, New York, **1985**, pp. 87–130.
[17] J. A. Ferguson, T. J. Meyer, *J. Chem. Soc. D* **1971**, 623–624.
[18] not available Trinh Toan, B. K. Teo, J. A. Ferguson, T. J. Meyer, L. F. Dahl, *J. Am. Chem. Soc.* **1977**, *99*, 408–416.
[19] H. Ogino, A. Satoh, M. Shimoi, *Bull. Chem. Soc. Jpn.* **1990**, *63*, 2314–2317.
[20] S.-B. Yu, G. C. Papaefthymiou, R. H. Holm, *Inorg. Chem.* **1991**, *30*, 3476–3485.
[21] H. Ogino, H. Tobita, K. Yanagisawa, M. Shimoi, C. Kabuto, *J. Am. Chem. Soc.* **1987**, *109*, 5847–5848.
[22] A. K. Verma, S. C. Lee, *J. Am. Chem. Soc.* **1999**, *121*, 10838–10839.
[23] A. K. Verma, T. N. Nazif, C. Achim, S. C. Lee, *J. Am. Chem. Soc.* **2000**, *122*, 11013–11014.
[24] H. Link, A. Decker, D. Fenske, *Z. Anorg. Allg. Chem.* **2000**, *626*, 1567–1574.
[25] J. S. Duncan, T. M. Nazif, A. K. Verma, S. C. Lee, *Inorg. Chem.* **2003**, *42*, 1211–1224.
[26] J. S. Duncan, M. J. Zdilla, S. C. Lee, *Inorg. Chem.* **2007**, *46*, 1071–1080.
[27] M. J. Zdilla, A. K. Verma, S. C. Lee, *Inorg. Chem.* **2011**, *50*, 1551–1562.
[28] X.-D. Chen, J. S. Duncan, A. K. Verma, S. C. Lee, *J. Am. Chem. Soc.* **2010**, *132*, 15884–15886.
[29] X.-D. Chen, J. S. Duncan, S. C. Lee, *Inorg. Chem.* **2012**, *51*, 12891–12904.
[30] C. Ting-Wah Chu, R. S. Gall, L. F. Dahl, *J. Am. Chem. Soc.* **1982**, *104*, 737–746.
[31] R. S. Gall, C. Ting-Wah Chu, L. F. Dahl, *J. Am. Chem. Soc.* **1974**, *96*, 4019–4023.
[32] J. A. Ferguson, T. J. Meyer, *J. Am. Chem. Soc.* **1972**, *94*, 3409–3412.
[33] M. D. Westmeyer, M. A. Massa, T. B. Rauchfuss, S. R. Wilson, *J. Am. Chem. Soc.* **1998**, *120*, 114–123.
[34] W.-Y. Yeh, H.-M. Chang, *Organometallics* **2009**, *28*, 5992–5997.
[35] J. M. Berg, R. H. Holm in *Iron-Sulfur Proteins* (Ed.: T. G. Spiro), Wiley-Interscience, New York, **1982**, pp. 1–66.
[36] S. C. Lee, W. Lo, R. H. Holm, *Chem. Rev.* **2014**, *114*, 3579–3600.
[37] H. Seino, M. Hidai, *Chem. Sci.* **2011**, *2*, 847–857.
[38] M. Vogt, B. de Bruin, H. Berke, M. Trincado, H. Grützmacher, *Chem. Sci.* **2011**, *2*, 723–727.
[39] C. Lichtenberg, L. Viciu, M. Adelhardt, J. Sutter, K. Meyer, B. de Bruin, H. Grützmacher, *Angew. Chem. Int. Ed.* **2015**, *54*, 5766–5771; *Angew. Chem.* **2015**, *127*, 5858–5863.
[40] K. Dehnicke, M. Krieger, W. Massa, *Coord. Chem. Rev.* **1999**, *182*, 19–65.
[41] E. J. Laskowski, R. B. Frankel, W. O. Gillum, G. C. Papaefthymiou, J. Renaud, J. A. Ibers, R. H. Holm, *J. Am. Chem. Soc.* **1978**, *100*, 5322–5337.
[42] K. B. Musgrave, H. C. Angove, B. K. Burgess, B. Hedman, K. O. Hodgson, *J. Am. Chem. Soc.* **1998**, *120*, 5325–5326.
[43] M. Chakrabarti, L. Deng, R. H. Holm, E. Münck, E. L. Bominar, *Inorg. Chem.* **2009**, *48*, 2735–2747.
[44] T. Büttner, J. Geier, G. Frison, J. Harmer, C. Calle, A. Schweiger, H. Schönberg, H. Grützmacher, *Science* **2005**, *307*, 235–238.

[45] N. Donati, D. Stein, T. Büttner, H. Schönberg, J. Harmer, S. Anadaram, H. Grützmacher, *Eur. J. Inorg. Chem.* **2008**, 4691–4703.

[46] Attempts to synthesize species $[Fe_4(Ntrop)_4]^{n-}$ $(n>1)$ by reaction of **1** with >1 equiv of strong reducing agents such as KC_8 or Na naphthalide were so far unsuccessful.

[47] The onset potential for reductive decomposition of THF is ca. −3.2 V in our setup, resulting in higher currents at E_3 and E_4 (Supporting Information). The peak separation at E_3 and E_4 are not smaller than those for E_1 and E_2; that is, E_3 and E_4 are unlikely to correspond to two-electron redox events.

[48] K. T. Potts, M. Keshavarz-K, F. S. Tham, H. D. Abruña, C. Arana, *Inorg. Chem.* **1993**, *32*, 4450–4456.

[49] J. G. Reynolds, C. L. Coyle, R. H. Holm, *J. Am. Chem. Soc.* **1980**, *102*, 4350–4355.

[50] H. Inoue, N. Fujimoto, E. Imoto, *J. Chem. Soc. Chem. Commun.* **1977**, 412–413.

[51] D. M. P. Mingos, D. J. Wales, *Introduction to Cluster Chemistry*, Prentice Hall, Englewood Cliffs, **1990**.

[52] C. T.-W. Chu, F. Y.-K. Lo, L. F. Dahl, *J. Am. Chem. Soc.* **1982**, *104*, 3409–3422.

[53] CCDC 1056421 (**1**), 1056422 (**2a**), and 1056423 (H_2Ntrop) contain the supplementary crystallographic data for this paper. These data are provided free of charge by The Cambridge Crystallographic Data Centre.

Received: June 19, 2015
Revised: July 20, 2015